

COSMIC MICROWAVE BACKGROUND–WEAK LENSING CORRELATION: ANALYTICAL AND NUMERICAL STUDY OF NON-LINEARITY AND IMPLICATIONS FOR DARK ENERGY

ATSUSHI J. NISHIZAWA¹, EIICHIRO KOMATSU², NAOKI YOSHIDA¹, RYUICHI TAKAHASHI¹, NAOSHI SUGIYAMA^{1,3}

Draft version October 26, 2018

ABSTRACT

Non-linear evolution of density fluctuations yields secondary anisotropies in the cosmic microwave background (CMB), which are correlated with the same density fluctuations that can be measured by weak lensing (WL) surveys. We study the CMB-WL correlation using analytical models as well as N -body simulations. We show that an analytical model based upon the time derivative of non-linear matter power spectrum agrees with simulations. All-sky cosmic-variance limited CMB and WL surveys allow us to measure the correlation from non-linearity with high significance (50σ) for $l_{\max} = 10^4$, whereas the forthcoming missions such as Planck and LSST are expected to yield only marginal detections. The CMB-WL correlation is sensitive to the time derivative of structure growth. We study how this property may be used to constrain the nature of dark energy. While the expected constraints are not very strong, they may provide a cross check of results from other observations.

Subject headings: cosmology: theory — large scale structure of universe — cosmic microwave background

1. INTRODUCTION

Secondary temperature anisotropies of the cosmic microwave background (CMB) provide invaluable information on the structure formation in the universe. The sources of anisotropies include the Sunyaev-Zel'dovich (SZ) effects by galaxy clusters as well as by reionization, the Rees-Sciama (RS) effect, and CMB lensing.

The forthcoming Planck satellite and ground-based observations such as Atacama Cosmology Telescope (ACT; Kosowsky 2003) and South-Pole Telescope (SPT; Ruhl et al. 2004) are designed to measure temperature fluctuations at arc-minute scales, and thus are expected to detect some of the secondary anisotropies.

The Rees-Sciama effect is, in principle, a unique probe of the *time-variation* of gravitational potential, as it is given by (Sachs & Wolfe 1967; Rees & Sciama 1968)

$$\frac{\Delta T(\hat{n})}{T} = 2 \int_0^{r_*} dr \Phi'(\hat{n}r, r), \quad (1)$$

where Φ is the Newtonian potential, \hat{n} is a unit direction vector, r is the conformal *lookback* time, and r_* is r out to the photon decoupling epoch. The prime denotes $\partial/\partial r$, which is equal to $-\partial/\partial\eta$, where η is the conformal time.

In the linear regime, Φ' vanishes in a matter-dominated universe; however, when either curvature or dark energy dominates, Φ decays in time and thus $|\Phi'| > 0$. In the *non-linear* regime, on the other hand, Φ *grows* in time, $|\Phi'| < 0$. Therefore, one expects $\Phi\Phi' > 0$ on large scales where density fluctuations are still linear, and $\Phi\Phi' < 0$ on small scales where fluctuations are non-linear.

The auto-correlation of the RS effect, both lin-

ear and non-linear, has been studied (Seljak 1996; Tuluie et al. 1996; Cooray 2002b). The cross-correlation between the *linear* RS effect and large-scale structure traced by galaxies has also been studied (e.g., Crittenden & Turok 1996; Peiris & Spergel 2000; Cooray 2002a; Afshordi 2004), and detected for various galaxy surveys (e.g., Boughn & Crittenden 2004; Nolta et al. 2004; Afshordi et al. 2004).

Much less attention has been given to the correlation of the *non-linear* RS effect and large-scale structure. As this effect changes the sign at the linear-to-non-linear transition scale, the signature of non-linearity is distinct.

The RS effect is not the only thing that is correlated with the large-scale structure. The SZ effects, as well as radio and infrared point sources, also trace the large-scale structure. Fortunately, multi-frequency data enable us to separate these contributions that have unique and specific frequency dependence.

In this paper, we calculate the cross-correlation of the RS effect and large-scale structure traced by weak lensing (WL) surveys. In particular, we simulate this directly using a N -body code for the first time.

We adopt the standard Λ CDM model with $(\Omega_{m0}, \Omega_{\Lambda0}, \sigma_8, h, n_s) = (0.26, 0.74, 0.76, 0.7, 1)$, which is consistent with Spergel et al. (2007).

2. ANALYTICAL MODEL

The amplitude of distortion in galaxy images due to WL is given by the so-called convergence, κ , which is proportional to the projected density field along the line of sight. As the Newtonian potential, Φ , is negatively proportional to density field via the Poisson equation, the sign of CMB-WL correlation is given by $-\Phi\Phi'$; thus, negative on large scales and positive on small scales.

The cross-correlation of the RS effect and κ , C_l , is

$$C_l = -2l^2 \int_0^{r_*} dr P_{\Phi\Phi'}(l/r; r) \int_z^{z_*} dz_s p(z_s) \frac{r_s - r}{r_s r^3}, \quad (2)$$

where $P_{\Phi\Phi'}(k; r)$ is the power spectrum of $\Phi\Phi'$ at r , z_s

arXiv:0711.1696v1 [astro-ph] 12 Nov 2007

Electronic address: atsushi@a.phys.nagoya-u.ac.jp

¹ Department of Physics, Nagoya University, Furocho, Nagoya, Aichi 464-8602, Japan

² Department of Astronomy, University of Texas at Austin, Austin, TX 78712 USA

³ Institute for Physics and Mathematics of the Universe, University of Tokyo, 5-1-5 Kashiwa-no-Ha, Kashiwa City, Chiba 277-8582, Japan

is the redshift of source galaxies, and $r_s \equiv r(z_s)$. Here, $p(z)dz$ is the probability of finding galaxies between z and $z + dz$. We use $p(z) = Az^2 \exp[-(z/z_0)^\beta]$, where A is a normalization factor determined by $\int_0^\infty p(z)dz = 1$ (Efstathiou et al. 1991). We consider two survey designs: (*Model 1*) Deep Survey, $(\beta, z_0) = (0.7, 0.5)$, whose $p(z)$ peaks at $z \sim 2.2$ with a broad distribution, and (*Model 2*) Shallow Survey, $(\beta, z_0) = (2, 0.9)$, which peaks at $z \simeq 0.9$ with a narrower distribution.

We calculate $P_{\Phi\Phi'}$ from

$$P_{\Phi\Phi'}(k, r) = \frac{9\Omega_{m0}^2 H_0^4}{4a^2 k^4} [P_{\delta\delta'}(k, r) - \mathcal{H}P_{\delta\delta}(k, r)], \quad (3)$$

where $\mathcal{H} = -d \ln a / dr$, and $P_{\delta\delta}$ and $P_{\delta\delta'}$ are the power spectrum of density fluctuations, δ , and the cross-correlation of δ and δ' , respectively.

How do we calculate $P_{\delta\delta'}$? The continuity equation, $\delta' = q$ where $q \equiv \nabla \cdot [\mathbf{v}(1 + \delta)]$ is the momentum divergence, gives the *exact* relation, $P_{\delta\delta'} = P_{\delta q}$. Here, $P_{\delta q}$ is the density-momentum divergence cross spectrum.

It might be tempting to use $P_{\delta\delta'} = P'_{\delta\delta}/2$, as the following might seem obvious: $\langle \delta_{\mathbf{k}}(r) \delta'_{\mathbf{p}}(r) \rangle = \frac{1}{2} \frac{\partial}{\partial r} \langle \delta_{\mathbf{k}}(r) \delta_{\mathbf{p}}(r) \rangle$. However, this relation is exact only in the linear regime, for which the ensemble average (taken over initial perturbations) and $\partial/\partial r$ commute. As they do not generally commute in the non-linear regime, we check whether this *ansatz* is a good approximation in the non-linear regime.

We test this *ansatz* by comparing $P_{\delta q}$ and $P'_{\delta\delta}/2$. We use the 3rd-order perturbation theory (PT), as it allows us to study this delicate issue analytically.

We expand $\delta_{\mathbf{k}}(r)$ in a series up to the 3rd order in the initial linear perturbation, $\delta_1(\mathbf{k})$, as $\delta_{\mathbf{k}}(r) = \sum_{n=1}^3 D^n(r) \delta_n(\mathbf{k})$. We also expand the velocity divergence, $\theta \equiv \nabla \cdot \mathbf{v}$, in Fourier space up to the 3rd order in the initial perturbation, $\theta_1(\mathbf{k})$, as $\theta_{\mathbf{k}}(r) = \sum_{n=1}^3 D'(r) D^{n-1}(r) \theta_n(\mathbf{k})$. Here, D is the linear growth factor, and δ_n and θ_n are of order δ_1^n and θ_1^n , respectively.

With this expansion, we obtain

$$\begin{aligned} P_{\delta q}(k, r) &= D(r)D'(r)P_{\delta\delta}^{11}(k) \\ &+ D^3(r)D'(r) [P_{\delta\theta}^{13}(k) + P_{\delta\theta}^{31}(k) + P_{\delta\theta}^{22}(k)] \\ &+ D^3(r)D'(r) \int \frac{d^3 p}{(2\pi)^3} \frac{\mathbf{k} \cdot \mathbf{p}}{p^2} [B_{\delta\theta\delta}^{112}(\mathbf{k}, \mathbf{p}) \\ &+ B_{\delta\theta\delta}^{121}(\mathbf{k}, \mathbf{p}) + B_{\delta\theta\delta}^{211}(\mathbf{k}, \mathbf{p})], \quad (4) \end{aligned}$$

where $P_{\delta\delta}^{11}(k)$ is the initial linear spectrum, $P_{\delta\theta}^{ij}(k)$ is the cross-correlation of δ_i and θ_j , and $B_{\delta\theta\delta}^{ijl}(\mathbf{k}, \mathbf{p}) \equiv \langle \delta_i(\mathbf{k} - \mathbf{p}) \theta_j(\mathbf{p}) \delta_l(\mathbf{k}) \rangle$, whose explicit forms can be calculated in a straightforward manner by following Scoccimarro (2004).

We then compare $P_{\delta q}$ with the 3rd order expression of $P'_{\delta\delta}/2$ (Bernardeau et al. 2002)

$$\begin{aligned} \frac{1}{2} P'_{\delta\delta}(k, r) &= D(r)D'(r)P_{\delta\delta}^{11}(k) \\ &+ 2D^3(r)D'(r)[P_{\delta\delta}^{22}(k) + 2P_{\delta\delta}^{13}(k)]. \quad (5) \end{aligned}$$

While equation (4) and (5) are obviously identical to the first-order, it is not immediately clear whether $P_{\delta q} = P'_{\delta\delta}/2$ holds in the non-linear regime. We find $P_{\delta q} \approx P'_{\delta\delta}/2$ to the accuracy better than 10% for $k < 1h/\text{Mpc}$, and 5% for $k < 0.4h/\text{Mpc}$, at $r = 0$.

In the right panel of Figure 1, we compare C_l calculated from $P_{\delta q}$ (dashed) and $P'_{\delta\delta}/2$ (solid). We find that, in the non-linear regime ($l \gtrsim 1000$) where the correlation turns positive, C_l from $P'_{\delta\delta}/2$ is smaller by $\sim 10\%$. This result suggests that we can use $P_{\delta\delta'} = P'_{\delta\delta}/2$ to compute $P_{\Phi\Phi'}$ from equation (3) reasonably accurately.

However, our argument is still limited to PT, which breaks down for $\delta \gtrsim 1$. In the same panel of Figure 1, the dotted lines show C_l from $P'_{\delta\delta}$, where $P_{\delta\delta}$ is the fully evolved non-linear power spectrum (Smith et al. 2003). The 3rd-order PT overestimates non-linearity in $P_{\delta\delta}$ (Bernardeau et al. 2002; Jeong & Komatsu 2006), and thus PT predicts that the sign of C_l changes at smaller l . This result shows limitations of PT.

3. ANALYTICAL MODEL VS N -BODY SIMULATION

To test $P_{\delta\delta'} \approx P'_{\delta\delta}/2$ in the non-linear regime, we compare the analytical model with N -body simulations.

We employ 512^3 dark matter particles in a volume of $L_{\text{box}} = 250h^{-1}\text{Mpc}$ and $40h^{-1}\text{Mpc}$ on a side. The simulations are performed by the GADGET-2 code (Springel 2005). The initial conditions are generated by a standard method using the Zel'dovich approximation. We dump outputs from $z = 0.01$ to 10 uniformly sampled in $\log(1+z)$. For each output redshift, we dump adjacent two outputs in order to calculate δ' and Φ' .

In the top left panel of Figure 1, we show the analytical model of C_l with Smith et al.'s $P_{\delta\delta}$ (solid and long-dashed show Model 1 and 2, respectively) and the N -body results (open and filled symbols show negative and positive values, respectively). The agreement is good: the model describes the amplitude, shape, and cross-over at $l \sim 800$ of C_l that are measured in the simulation. We therefore conclude that the *ansatz*, $P_{\delta\delta'} \approx P'_{\delta\delta}/2$, is indeed accurate, up to $l = 5000$ where we can trust resolution of our N -body simulation.

How well are RS and WL correlated? In the bottom left panel of Figure 1, we show the 2-d correlation coefficient, $R_l = C_l / \sqrt{C_l^{\kappa} C_l^{RS}}$. We have used the same non-linear $P_{\delta\delta}$ to calculate the power spectrum of convergence, C_l^{κ} , while we have used the halo model approach (Cooray & Sheth 2002) to calculate that of RS, C_l^{RS} . The RS and κ are strongly anti-correlated, $R_l \simeq -1$, in the linear regime. (It is not exactly -1 because of the projection effect.) The correlation weakens as non-linearity becomes important: $R_l \simeq 0.05 - 0.1$ at $10^3 \lesssim l \lesssim 10^4$ for Deep (Model 1), and $R_l \simeq 0.01 - 0.03$ for Shallow (Model 2).

The weak correlation of C_l is due to the fact that Φ and Φ' are not correlated very well in the non-linear regime: the 3-d correlation coefficient, $R_{3D}(k) = P_{\Phi\Phi'}(k) / \sqrt{P_{\Phi}(k)P_{\Phi'}(k)}$, reaches the maximal value, $R_{3D}(0.5\text{Mpc}) \simeq 0.2$, at $z = 1$, where the RS effect becomes largest. The 2-d correlation, R_l , is even weaker than $R_{3D}(k)$ because of the projection effect and a mismatch between the redshift at which WL becomes largest ($z \simeq 0.5$) and that for RS ($z \simeq 1$).

The weak correlation makes it challenging to measure the CMB-WL correlation from non-linearity.

4. DETECTING NON-LINEAR REES-SCIAMA EFFECT

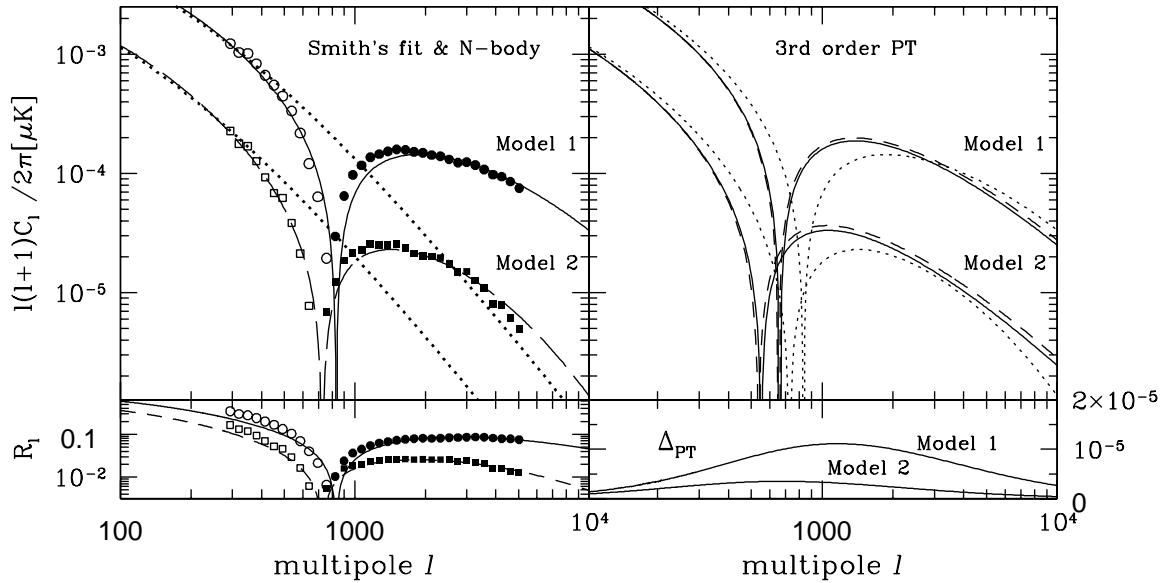


FIG. 1.— CMB-WL cross-correlation spectra, C_l , for two WL survey designs: Deep (Model 1) and Shallow (Model 2). (Top left) The symbols show C_l from the N -body simulation. The open and filled symbols show $C_l < 0$ and $C_l > 0$, respectively. The solid and long-dashed lines show the fully non-linear model for Model 1 and 2, respectively, while the dotted lines show the linear theory predictions. Note that the linear theory predicts $C_l < 0$ at all l . (Bottom left) CMB-WL cross-correlation coefficients, R_l . (Top right) 3rd-order PT predictions. The solid and dashed lines show two ways of calculating C_l , based upon Eq. (5) and (4), respectively. The fully non-linear calculations are also shown as the dotted lines (which are exactly the same as the solid and long-dashed lines on the top-left panel). (Bottom right) Difference between two ways of calculating C_l . The fractional differences are at most $\sim 10\%$.

Can we detect non-linearity, $C_l > 0$? The signal-to-noise ratio (S/N) of C_l is given by

$$\left(\frac{S}{N}\right)_{l_{\max}}^2 = f_{\text{sky}} \sum_{l=2}^{l_{\max}} \frac{2l+1}{1 + (\tilde{C}_l^{\text{CMB}} \tilde{C}_l^{\kappa} / C_l^2)}, \quad (6)$$

where f_{sky} is the fraction of sky observed, and \tilde{C}_l^{CMB} and \tilde{C}_l^{κ} are the total (signal plus noise) power spectra of CMB (including primary, CMB lensing and RS) and WL, respectively. The noise spectra of CMB and WL surveys are given, respectively, by (Knox 1995; Schneider 2005)

$$N_l^{\text{CMB}} = \sigma_{\text{pix}}^2 \theta_{\text{fwhm}}^2 \exp[l(l+1)\theta_{\text{fwhm}}^2/8 \ln 2], \quad (7)$$

$$N_l^{\kappa} = \sigma_{\gamma}^2 / n_{\text{gal}}, \quad (8)$$

where σ_{pix} is the temperature noise per pixel, θ_{fwhm} is the FWHM of a Gaussian beam, n_{gal} is the number density of galaxies observed in a WL survey, and σ_{γ} is the noise in shear measurements, including intrinsic ellipticities.

We forecast S/N for the forthcoming surveys with the following parameters: $(f_{\text{sky}}, \sigma_{\gamma}, n_g/\text{arcmin}^2) = (0.024, 0.3, 20)$ for Canada-France-Hawaii Telescope Legacy Survey (CFHTLS), $(0.8, 0.1, 100)$ for Large Synoptic Survey Telescope (LSST), $(f_{\text{sky}}, \sigma_{\text{pix}}, \theta_{\text{FWHM}}) = (0.024, 4.4\mu\text{K}, 1'.7)$ for ACT, and $(0.8, 1.7/2/4/3\mu\text{K}, 10'.7/8'/5'.5)$ for Planck with 3 channels.

In Figure 2, we show the predicted S/N as a function of the maximum multipole, l_{\max} , for cosmic-variance limited CMB and WL (Deep and Shallow) surveys, as well as for the forthcoming surveys: Planck correlated with LSST, and ACT correlated with CFHTLS.

We find that S/N is totally dominated by the linear contribution (dotted lines) at $l \lesssim 3000$, and then becomes dominated by the non-linear contribution (dashed lines) at higher l . All-sky CMB and WL surveys can yield

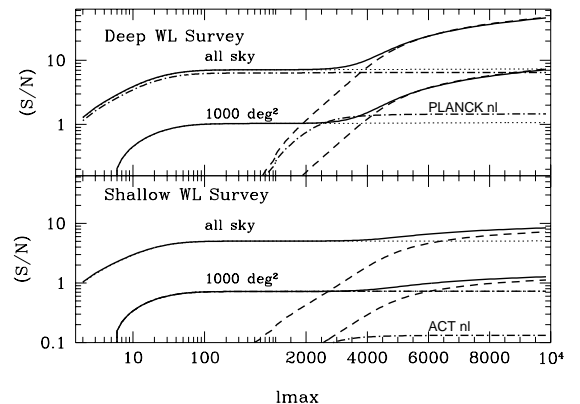


FIG. 2.— Signal-to-noise ratio (S/N) as a function of the maximum multipole, l_{\max} . The dotted and dashed lines show the linear and non-linear contributions, respectively, while the solid lines show the total, for cosmic-variance limited CMB and WL surveys with all-sky (upper curves) and 1000-deg² sky coverage (lower curves). (Top) Deep WL Survey. The dashed-dotted lines show S/N expected from Planck's CMB data correlated with LSST's WL data. "PLANCK nl" shows the non-linear contribution only. (Bottom) Shallow WL Survey. Same as the top panel, but for ACT's CMB data correlated with CFHTLS's WL data.

$S/N \sim 50$ (10) for Deep (Shallow) WL Survey, whereas 1000 deg² surveys can only yield $S/N \sim 7$ (1).

Once noise of the forthcoming surveys is included, however, S/N from the non-linear contribution becomes small compared to the linear contribution. For Planck+LSST we find $S/N \sim 1.5$ for the non-linear, and 6 for the linear. For ACT+CFHTLS we find $S/N \sim 0.1$ for the non-linear, and 0.7 for the linear. Therefore, we conclude that these forthcoming surveys are not expected to yield significant detection of non-linear RS effect.

5. SENSITIVITY TO DARK ENERGY PARAMETERS

As the linear RS effect vanishes during the matter era, it is sensitive to dark energy (DE) (e.g., Boughn & Crittenden 2004; Nolta et al. 2004; Afshordi et al. 2004). The non-linear effect measures the structure growth, which is also sensitive to DE (Verde & Spergel 2002). The cross-over at $l \sim 800$, at which the linear and non-linear contributions cancel, is particularly a unique probe of DE.

The top panels of Figure 3 show sensitivity of C_l to DE parameters: $\partial C_l/\partial\Omega_{\Lambda 0}$, $\partial C_l/\partial w_0$, and $\partial C_l/\partial w_1$. We use a simple form of DE equation of state, $w(a) = p_{\Lambda}(a)/\rho_{\Lambda}(a)$, given by $w(a) = w_0 + w_1(1 - a)$. The fiducial values are $w_0 = -1$ and $w_1 = 0$.

We find $\partial C_l/\partial w_0 < 0$ and $\partial C_l/\partial w_1 < 0$ at all l . By increasing w_0 or w_1 , one makes $w(a)$ less negative which, in turn, makes DE more important at earlier times. This does two things. On large scales where $C_l < 0$, it enhances the linear RS effect, making C_l even more negative. On small scales where $C_l > 0$, it reduces the growth of non-linear structure, making C_l less positive. In both cases we find negative derivatives.

Dependence on $\Omega_{\Lambda 0}$ is more complex. While $\partial C_l/\partial\Omega_{\Lambda 0} < 0$ at most l can be explained by the same physics as above, we find $\partial C_l/\partial\Omega_{\Lambda 0} > 0$ in the intermediate l . This is due to the assumption of a flat universe: a larger $\Omega_{\Lambda 0}$ results in a smaller Ω_{m0} , which alters the shape of $P_{\delta\delta}(k)$ by shifting it to larger scales. (A smaller Ω_{m0} delays matter-radiation equality.) This shift causes the intermediate l to behave differently. The behavior in the intermediate l has little to do with non-linearity, as we observe the same effect in the linear prediction.

Having evaluated the derivatives, we use the Fisher matrix analysis to calculate the expected constraints on DE parameters, $p_{\alpha} = (\Omega_{\Lambda 0}, w_0, w_1)$, from the CMB-WL correlation. The Fisher matrix is given by $F_{\alpha\beta} = \sum_{l=2}^{l_{\max}} (\partial C_l/\partial p_{\alpha}) \text{Cov}^{-1} (\partial C_l/\partial p_{\beta})$ where Cov is the covariance matrix (Eq. 6) and $l_{\max} = 10^4$.

The bottom panel of Figure 3 shows the expected joint constraints on w_0 and w_1 from C_l of all-sky cosmic-variance limited CMB and WL surveys. When $\Omega_{\Lambda 0}$ is not marginalized but fixed at the fiducial value, we find $w_0 = -1 \pm 1.1$ (0.4) and $w_1 = 0 \pm 4.1$ (1.1) for Shallow (Deep) WL Survey. The constraints are not very strong, unfortunately; however, the direction of degeneracy line, $w_1 \simeq 2(w_0 + 1)$, is about twice as steep as that of a joint analysis of the baryon oscillations and Type Ia supernovae observations (Seo & Eisenstein 2003).

6. CONCLUSION

We have studied the cross-correlation between CMB (the RS effect) and large-scale structure traced by WL. We have developed a simple analytical model based upon the time derivative of non-linear matter power spectrum, and tested its validity analytically with 3rd-order PT as

well as numerically with N -body simulations.

We have shown that all-sky cosmic-variance limited CMB and deep (shallow) WL surveys can yield a 50σ (10σ) detection of the *non-linear* CMB-WL correlation for $l_{\max} = 10^4$. The forthcoming surveys are not expected to yield significant detections. We expect $\sim 1.5\sigma$ from Planck+LSST and 0.1σ from ACT+CFHTLS.

The change of the sign of C_l at the cross-over, $l \sim 800$, offers a unique probe of the nature of DE. Sensitivity

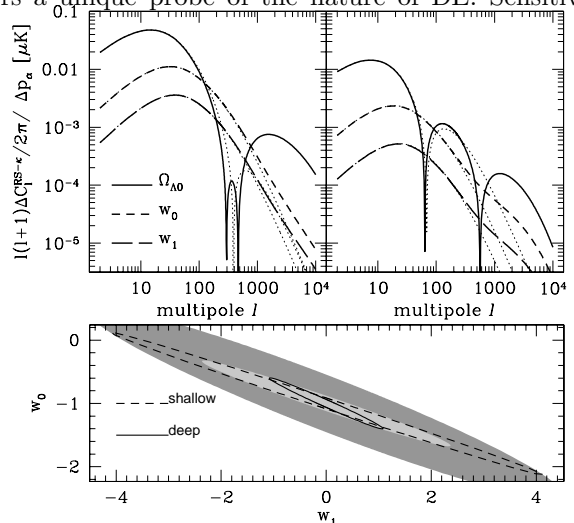


FIG. 3.— Sensitivity of the CMB-WL correlation to dark energy (DE). (Top) Derivatives of C_l with respect to the DE parameters. The solid, short-dashed, and long-dashed curves show $\partial C_l/\partial\Omega_{\Lambda 0}$, $\partial C_l/\partial w_0$, and $\partial C_l/\partial w_1$, respectively. The thin dotted lines show those from linear theory. (Bottom) Fisher matrix forecasts for all-sky cosmic-variance limited CMB and WL surveys. The light and dark areas show the expected $1\text{-}\sigma$ constraints from Deep and Shallow WL Surveys, respectively, with $\Omega_{\Lambda 0}$ marginalized. The solid and dashed lines show the same things with $\Omega_{\Lambda 0}$ fixed.

of the CMB-WL correlation to DE turns out to be not very strong; however, as the direction of degeneracy on $w_0 - w_1$ is different from that of the baryon oscillations and Type Ia supernovae, it may provide an independent cross-check of the results from these observations.

ACKNOWLEDGMENTS

We thank Olivier Doré, Joe Hennawi, Ravi Sheth, and David Spergel for useful discussions and comments on the paper. The work is supported by Grant-in-Aid for Scientific Research on Priority Areas No. 467 “Probing the Dark Energy through an Extremely Wide & Deep Survey with Subaru Telescope” and by The Mitsubishi Foundation. The numerical computation is done by cluster computers in Nagoya University. EK acknowledges support from an Alfred P. Sloan Fellowship.

REFERENCES

- Afshordi, N. 2004, Phys. Rev. D, 70, 083536
 Afshordi, N., Loh, Y., & Strauss, M. 2004, Phys. Rev. D, 69, 083524
 Bernardeau, F., Colombi, S., Gaztanaga, E., & Scoccimarro, R. 2002, Phys. Rept., 367, 1
 Boughn, S., & Crittenden, R. 2004, Nature, 427, 45
 Cooray, A. 2002a, Phys. Rev. D, 65, 103510
 Cooray, A. 2002b, Phys. Rev. D, 65, 083518
 Cooray, A., & Sheth, R. K. 2002, Phys. Rept., 372, 1
 Crittenden, R. G., & Turok, N. 1996, Phys. Rev. Lett., 76, 575
 Efstathiou, G., Bernstein, G., Tyson, J. A., Katz, N., & Guhathakurta, P. 1991, ApJ, 380, L47
 Jeong, D., & Komatsu, E. 2006, ApJ, 651, 619
 Knox, L. 1995, Phys. Rev. D, 52, 4307
 Kosowsky, A. 2003, New Astronomy Review, 47, 939
 Nolta, M. R., et al. 2004, ApJ, 608, 10

- Peiris, H. V., & Spergel, D. N. 2000, ApJ, 540, 605
Rees, M., & Sciama, D. 1968, Nature, 217, 511
Ruhl, J., et al. 2004, SPIE, 5498, 11
Sachs, R., & Wolfe, A. 1967, ApJ, 147, 73
Schneider, P. 2005, astro-ph, 0509252
Soccimarro, R. 2004, Phys. Rev. D, 70, 083007
Seljak, U. 1996, ApJ, 460, 549
Seo, H.-J., & Eisenstein, D. J. 2003, ApJ, 598, 720
Smith, R. E., et al. 2003, MNRAS, 341, 1311
Spergel, D. N., et al. 2007, ApJS, 170, 377
Springel, V. 2005, MNRAS, 364, 1105
Tuluie, R., Laguna, P., & Anninos, P. 1996, ApJ, 463, 15
Verde, L., & Spergel, D. 2002, Phys. Rev. D, 65, 043007